Development of a model for calculating the solar ultraviolet Protection Factor of small to medium sized built shade structures

Alfio V. Parisi[1,*], Abdurazaq Amar[1], Nathan J. Downs[1,2], Damien P. Igoe[1], Simone L. Harrison[2,1,3] and Joanna Turner[1]

[1]Faculty of Health, Engineering and Sciences, University of Southern Queensland, Toowoomba, Australia.

[2]Skin Cancer Research Unit, College of Public Health, Medical and Veterinary Sciences, James Cook University, Townsville, Australia.

[3]College of Medicine and Dentistry, James Cook University, Townsville, Australia.

[*]To whom correspondence is to be addressed. Email: Alfio.Parisi@usq.edu.au.
Ph:+61 7 46312226

Abstract

A method was proposed for calculating the ultraviolet protection factor (PF) of small to medium built shade structures. The method takes into account the amount of sky view visible from under the structure, the transmittance of the roof material, the relative amount of diffuse ultraviolet radiation (UV), the measurement position under the structure and the albedo of the relevant surfaces. The PF of four different shade structure designs was measured 90 cm above ground-level at the centre of the widest diameter of each structure. Measurements were only made on cloud-free days. Three structures had a thin metal roof and the fourth had shade-cloth. The proportion of sky view ranged from 4.6% to 15.4% for these structures. The influence of position was investigated for one structure, with the PF evaluated 50 cm in from each of the sides at 90 cm above ground-level. The reliability of the method was tested by comparing calculated and measured PF values for solar zenith angles ranging from 7^{o} to 49^{o}. The mean absolute difference between the calculated and the measured PF for these small to medium structures was 1.4 PF (14%). The proposed method is more likely to be widely used to measure the PF *in situ* compared to measuring UV in full sun and in the shade with a UV meter because many stakeholders do not have access to UV meters due to the cost or the degree of specialization required to use these meters effectively.

Keywords: shade; PF; ultraviolet protection factor; erythemal UV; shade structures

1. Introduction

Excessive sun-exposure is the main environmental risk-factor for skin cancer; the most prevalent form of cancer in Caucasian populations. The risk of skin cancer can be minimized, with the World Health Organisation (WHO) stating that four out of five skin cancers are preventable [1]. Skin cancer poses a significant economic burden globally [2]. For instance in 2017, 13,941 cases of melanoma were diagnosed in Australia (average lifetime cost 44,796 AUD per case in 2010; [2, 3]), with the cost of keratinocyte cancers in 2012 estimated to be 703 AUD million and over 70 million for melanoma [4]. In the USA, 91,270 melanoma cases are expected in 2018 [5], with the cost of skin cancer treatments in the USA based on 2004 data being an estimated two billion dollars per year and solar keratoses adding a further $1.2 billion [6].

The primary prevention of skin cancer through reduced exposure to ultraviolet radiation (UV) will reduce the global burden of disease [7], associated health care expenditure [8] and the societal burden it poses. One essential component of a strategy to reduce UV exposure that is promoted by Cancer Council, Australia and WHO is the use of shade while outdoors [1, 9]. Previous research has reported that adequate protection is provided by those shade structures with an UV protection factor of 15 or more [10].

To assist the general public to determine whether a shade structure provides adequate UV protection, the UV protection factor (PF) of built shade structures which assesses the ratio of available incident solar radiation to the solar radiation with a shade structure in place, should be made available for public scrutiny. The Australian Standard AS 4174:2018 for knitted and woven shade fabrics only provides a method for determining in the laboratory the UV transmittance and the cover factor or percentage absorbance at 350 nm of shade-cloth and fabrics used on the roof of

structures such as shade sails. The Standard determines the attenuation of direct UV for new, dry, non-stretched materials, whereas the UV protection provided by shade-cloth roofing materials *in situ* is also influenced by the amount of stretch, and age of the roof material. The protection factor measured in the laboratory is significantly different to the protection factor provided by a shade structure once erected in a local environment due to the additional contribution of the diffuse UV component. Previous research has shown that the UV transmittance of the material used on the roof of structures purposefully built for the provision of shade is a poor indication of the actual PF of the built shade structure due to the other influencing factors such as surroundings, the position under the structure, roof materials and the amount of sky view from underneath the structure [11, 12]. A design of a shade structure using louvers that takes into account the angle of the sun to shade from the direct (shadow causing) UV radiation has been reported [13]. It is well established that both the direct and diffuse components of solar UV radiation contribute to human UV exposure [14] and the exposure due to the diffuse UV needs to be taken into account. Shade structures that only provide protection from direct solar UV alone, but do not block sufficient amounts of sky allowing exposure to diffuse solar UV radiation under the shade canopy, can have poor PF ratings [15]. Previous research has reported on the determination of the Sky View Factor (SVF) from Google Street View for larger scale urban settings [16-19]. The method presented here takes into account the SVF or sky view visible from under the structure, the UV transmittance of the roof material which may be rated in accordance with the Ultraviolet Effectiveness Classification (Australian Standard AS 4174:2018) [20], the relative amount of diffuse UV, the measurement position under the structure and the albedo of the relevant surfaces beneath the structure.

Some of the approaches used to evaluate the protection provided by shade structures previously have included shade audits [21-23], using software to map existing or proposed shade [24] and physical measurements of the PF of different types of shade [25-31]. Additionally, there are existing recommendations for shade provision [32-34].

Shade is a practical form of passive sun-protection that is particularly beneficial in schools since children and adolescents often resist wearing hats [35]. School students often seek shade during scheduled meal breaks to provide respite from the heat [36]. Similarly, in urban environments shading has been reported to provide thermal comfort [37-39]. Numerous people can utilize shade structures simultaneously and since these structures can be constructed with quality, durable materials to protect against weathering and everyday use, shade provision can be a cost-effective, enduring option for the school environment, complimenting existing strategies for minimizing UV exposure. Shade is particularly beneficial during lesson breaks and scheduled outdoor classes, such as physical education lessons, since these can coincide with peak UV exposure periods. The importance of shade provision as a sun-protection strategy is reflected in the distribution of shade grants to schools and non-profit organisations [40, 41].

Previous research [42] and a recent article by Choice [43] have reported on problems associated with not having a suitable means of communicating the PF of built shade structures to the public. For example, an opaque roof constructed from roofing material with a UV transmission of zero may offer inadequate UV protection (i.e. a PF of ~1.5 to 3) once the shade structure is erected [44, 45]. Others have reported on the inadequacy of UV protection provided by built structures at swimming pools with PFs ranging from 2 to 16 [11] and PFs of 4 to 8 for structures in a school

environment [30]. Utrillas *et al*., [46] proposed a method to measure the *in situ* PF of a shade umbrella, however there is currently no agreed means of determining the PF of the many and varied forms of shade structures both in Australia and abroad without a UV detector. This research reports on the development and validation of an accessible new tool for determining the *in situ* PF of small to medium sized built free-standing shade structures and provides useful insights for shade builders and consumers.

2. Methodology

A series of four free-standing built shade structures comprised of a small, a medium and a large structure all with solid thin metal roofs and a fourth structure with a shade-cloth roof (Figure 1) were used to develop and validate the proposed PF model. These four structures were selected because they are representative of the built shade structures currently found in parks managed by local government authorities in Australia. They were selected to provide typical examples of a range of different sized structures (small, medium and large) with a solid roof, as well as a typical free-standing shade-cloth structure. No adjacent buildings were located in the immediate vicinity of any of these built shade structures. All four free-standing built shade structures were located in the regional city of Toowoomba (27.6° S, 151.9° E) in Queensland, Australia. The physical dimensions of these structures are provided in Table 1.

Previous research has shown that the measured PF of a tree canopy was influenced by the presence of more than 50% cloud cover [47]. As this may be the case for shade structures, measurements supporting the development and validation of the PF were undertaken on cloud-free days to minimize the potential influence of cloud cover.

137 The proposed method is based on the proportion of sky view visible from beneath the structure,
138 the UV transmittance of the roof material, the relative proportion of available diffuse erythemal
139 UV and the albedo of the relevant surfaces beneath the structure. To calculate the proportion of
140 the sky view and the proportion of the sky covered by the roofing material of each of the structures,
141 wide-angle images were taken on a cloud-free day from a point in the centre of the structure, at 90
142 cm above ground-level, at approximately noon, and also between mid-morning and noon. Image
143 analysis was used to calculate the proportion of sky view and the proportion of the sky covered by
144 the roof for each structure. Additionally, as the PF can be influenced by the solar zenith angle
145 (SZA) [48], the PF model was evaluated for a range of SZAs from 7^{o} to 49^{o} [49]. Data on the
146 proportion of the sky view and the proportion of the sky covered by the roof of each structure were
147 entered into a model designed to calculate the erythemal UV beneath built shade structures. The
148 PF was then determined as described in Section 2.2.
149

Figure 1 - The four structures investigated included: (top left) a small structure, (top right) a large shade structure, (bottom left), a medium shade structure (bottom left), all with thin metal roofs except (bottom right), structure with shade-cloth roof.

Images were taken with a smartphone (Sony Xperia Z1, Sony Corporation, Tokyo, Japan) fitted with a fish eye lens (Oldshark, Fisheye 235 degrees lens, supplier: MiniInTheBox.com). Any make or model of smartphone would suffice. The phone was positioned on a horizontal plane 90 cm above ground-level with the camera pointing upwards. This height was chosen as some structures have a table at approximately 90 cm above the ground. The lens is supplied with a clip that makes it relatively easy to attach over the camera of a smartphone. A shutter control connected by Bluetooth (Bluetooth remote shutter, supplier: Kogan.com) was used to take the images to ensure the user was not in the field of view. The image focus was set as the underside of the structure roof directly above the smartphone camera (f/2.4) and the default settings for shutter speed (between 1/1,294 and 1/281 seconds) and ISO (32) were used.

2.1 Image Analysis

The images produced by the lens were larger than the camera sensor [50] resulting in approximately one third of the sky view of the image not being recorded for images taken at 90 cm above the ground. As the missing portion of the image was near the perimeter of the image, and generally included part of the sky view, it was necessary to calculate the complete amount of sky view visible. Although this problem could be overcome by using an expensive DLSR camera with an 8 mm fish eye lens, the cost would be prohibitive, making the proposed method for determining the PF of built shade accessible to fewer people. Rather, we opted to resolve this using relatively inexpensive and widely available tools. The smartphone fitted with the fish eye lens was set to video mode and placed in the centre of a turntable mounted on a tripod. The smartphone video camera was used to record the underside of each structure while the turntable was rotated through 360 degrees. For each structure, four video frames depicting the roof at 90 degree intervals were downloaded to a computer and photo-stitched together using free Image Composite Editor software [51] to produce a hemispherical photograph (Figure 2).

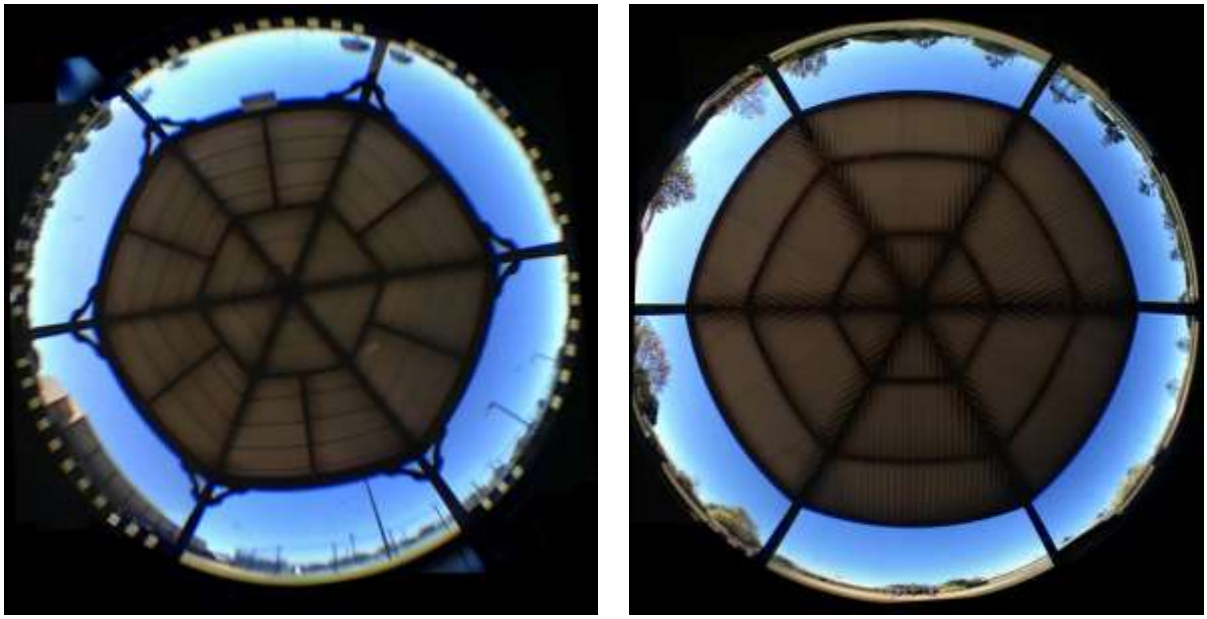

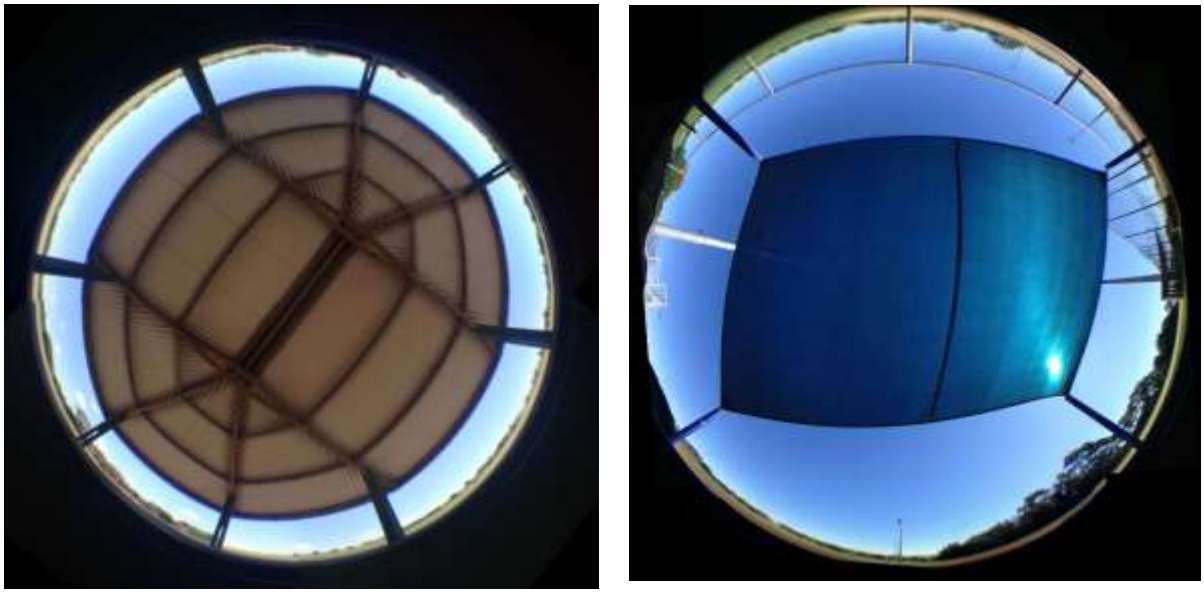

Figure 2 - Images taken 90 cm above ground-level with a smartphone fitted with a fish eye lens then photo-stitched to provide a complete image from beneath the structure for the (top left) small shade structure, (top right) medium shade structure, (bottom left), large shade structure and (bottom right) shade-cloth structure.

The proportion of sky view visible within each image was determined using the freely-available SVF Calculator software [52] which requires the royalty-free MATLAB Compiler Runtime [53] to be installed on a personal computer. This enables novice users to run the model without requiring a MATLAB license or programming skills.

The SVF Calculator segments the image into a series of annuli to calculate the SVF [54, 55]. After loading a hemispherical image of a shade structure, users specify the radius by clicking three points on the circumference. The software converts the image to black and white and automatically sets a threshold to distinguish between sky and non-sky pixels (including the structure's roof, supports, and surface objects). The threshold can be manually increased or decreased with a sliding bar. Any

non-sky pixels still incorrectly classified as sky, can be manually set to non-sky by selecting the relevant part of the image. The software then calculates SVF as a number between 0 and 1 (i.e. 0-100%).

Table 1 – Physical characteristics of four built shade structures typical of those found in parks in Toowoomba, Queensland (27.6° S, 151.9° E).

	Height (maximum height) (m)	Dimensions	Roof type (Transmittance)	Roof material albedo (%)	Ground cover	Albedo¶ (%)
Six sided small structure or gazebo	2.0 (2.7)*	3.5 m x 3.0 m Hexagon side length of 1.75 m	Metal (0%)	7.5	Pavers	9.2
Medium structure	2.05 (3.3)*	4.3 m x 3.7 m Hexagon, side length of 2.15 m	Metal (0%)	7.5	Concrete	9.2
Large structure	2.10 (2.85)*	5.75 m x 4.06 m Elongated octagonal shape	Metal (0%)	7.5	Concrete with large wooden table	4.0
Shade-cloth structure	2.0# (3.2)	6.6 m x 4 m	Shade-cloth (6%)	4.0	Grass	2.4

*Height measured at the edges and maximum height shown in brackets is the height at the apex.

Height is the minimum height of the structure.

¶ The albedo expressed as a percentage is the albedo of the ground cover beneath the structure as used in the model.

2.2 Protection Factor

The Protection Factor to a horizontal plane of a built structure is [11]:

$$PF = \frac{UVBE_{Global}}{UVBE_{Shade}} \quad (1)$$

where $UVBE_{Global}$ is the erythemally weighted UV irradiance [56] to a horizontal plane in full sun and $UVBE_{Shade}$ is the erythemally weighted UV irradiance to a horizontal plane beneath a shade structure.

For the PF model developed in this research for shade structures, the $UVBE_{Shade}$ was calculated using a modification for shade structures based on an approach reported for the calculation of the $UVBE_{Shade}$ under tree canopies [57]:

$$UVBE_{Shade} = \left(UV_{Diffuse} \times F_{Sky}\right) + \left(UV_{Global} \times F_{Roof} \times T\right) + \left(UV_{Diffuse} \times F_{Roof} \times \alpha_{Ground}\left(\frac{1}{2} + \alpha_{Roof}\right)\right) \quad (2)$$

where $UV_{Diffuse}$ is the diffuse horizontal plane erythemal UV, UV_{Global} is the global horizontal plane erythemal UV, F_{Sky} is the unobscured sky view fraction due to the shade structure for the particular measurement position within the shade, F_{Roof} is the sky view fraction obscured by the roof, T is the transmittance of the shade structure roof material in the erythemal UV waveband, α_{Ground} is the albedo of the ground beneath the structure and α_{Roof} is the albedo of the underside of the roof material. The third term of this equation represents the diffuse UV scattered from the ground surface under the structure and does not include the direct UV as that has been blocked by the roof of the shade structure. In this term, the α_{Roof} term is to take into account the UV scattered from the ground and then scattered by the roof to the receiving plane. The term with the factor of one half is to take into account the UV scattered from the ground and then undergoes scattering by the air molecules. One half is used on the assumption that half is scattered upwards and half is scattered downwards.

The albedo [58-61] of the various types of ground cover shown in Table 1 were used in these calculations of $UVBE_{Shade}$, along with the albedo of the underside of the roof material as reported in the literature [61] and as measured by the first author for the shade cloth structure The magnitude of the albedo's influence on the calculated PF is less than the influence due to the sky view. The influence of albedo was investigated for the small structure by testing albedo values of 7% and 11% in Equations (1) and (2) and comparing the resulting PFs (10.2, and 8.8, respectively) to that obtained with the 9.2% used in this model (PF 9.4). In both cases, calculated PF was within 1 PF of that calculated using the 9.2% albedo.

The transmittance in the erythemal UV waveband of the roof material was zero for the structures with the thin metal roof. For the shade-cloth roof, the erythemal UV transmittance employed was 6% where the supplier had provided this transmittance on their documentation for ten year old shade sail material (http://www.sunsetcanvas.com.au/products/shade/shade-sails).

The model PRO6UV [62] was used to calculate the $UVBE_{Global}$ and the $UVBE_{Diffuse}$ horizontal plane irradiances for cloud free days. The inputs to the model include latitude, longitude, elevation above sea level, time of day, day of year, albedo, aerosol optical depth and total column ozone. Similar models such as libRadtran [63] can be used. Calculated PF values were compared to values determined by measurements of $UVBE_{Global}$ and $UVBE_{Shade}$ with an erythemal UV meter (model 3D, Solar Light Co., PA, USA). $UVBE_{Shade}$ was measured on a horizontal plane in the centre of each shade structure from a position 90 cm above ground-level and equation (1) was used to determine the PF. The method was validated by conducting a series of $UVBE_{Global}$, and $UVBE_{Shade}$

measurements on cloud-free days for SZAs ranging from 9^{o} (summer - 24th, 25th and 31st January 2017; 15th and 16th January 2018) to 49^{o} (late autumn – 3rd, 11th, 16th and 29th May 2017).

2.3 Influence of Position Under Structure

The proposed model was used to determine the influence position beneath the structure had on *in situ* PF using PF determined from a central position beneath the small structure and 50 cm in from each of the six sides of the hexagonal structure on a cloud free day at approximately noon for an SZA of 16^{o}. Sky view fractions were measured for the north, north-east, south-east, south, south-west and north-western sides of the hexagonal structure. These data were also used to validate the model by comparing the calculated PF with the measured PF of the built shade structure.

3. Results and Discussion

3.1 Image Analysis

A photo-stitched image was generated for each shade structure using the images taken under each structure at a height 90 cm above ground-level using the smartphone fitted with the fish eye lens (Figure 2). The advantage of the proposed method is that smartphones are widely available and a fish eye lens similar to that used in this research is relatively inexpensive at less than 25 AUD. The amount of the sky view obstructed by each structure's roof and supports are visible in each image, together with any trees in the vicinity. The shade structure with the shade-cloth roof depicts a bright spot on the roof due to the partial transmission of direct sunlight. The proportion of SVF visible for each of the structures has been provided in (Figure 3), with the SVF ranging from 0.26 (26%) for the shade-cloth structure to 0.15 (15%) for the small structure to 0.05 (5%) for the large structure.

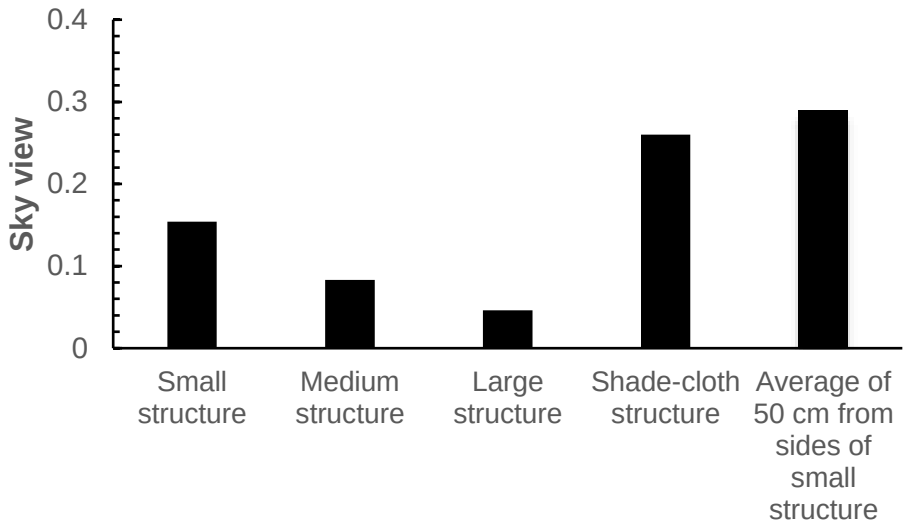

Figure 3 – Measured sky view beneath the centre of each of the four shade-structures at a height 90 cm above ground-level. The last column depicts sky view measured 50 cm in from the outer edge of the roof, averaged for the six sides of the small hexagon structure.

The average SVFs determined 50 cm in from each of the six sides of the small structure and 90 cm above ground-level was 0.289 (28.9%). SVFs determined 50 cm from the edge of the structure are almost double those obtained at the centre of the structure, demonstrating how the SVF of a structure varies with position under the structure. Our proposed technique enables PF to be determined at different positions under the structure.

3.2 Protection Factor

A comparison of the measured and the calculated irradiances for the global and the diffuse erythemal UV and the measured and calculated PFs for the three small to medium structures determined on cloud free days are provided in Figure 4. The resulting 1:1 lines are drawn in the figure for comparison. PFs are likely to be lower on cloudy days due to the increased relative amount of diffuse UV. PFs varied from approximately 5 for the small structure to 15 for the medium structure for the SZA at the time of the PF calculation. For the sides of the small structure,

SVFs determined 50 cm from the edge of the small structure ranged from 0.23 to 0.38, compared to 0.11 for the same structure measured in the centre. The resulting PFs for the same structure evaluated on a cloud free day were lower at the edge (ranged from 5 to 8) than at the centre (9 to 11), illustrating how the PF of a shade structure changes according to the measurement position beneath the structure.

This research was not designed to compare the PFs of different shade structures, but rather to develop and propose an accessible method by which PF could be calculated, given that the PF changes with SZA and position within the structure. The mean absolute error (MAE) or mean absolute difference between calculated and measured erythemal UV irradiances was 0.02 W/m^2 (13%). The MAE between the calculated and measured PFs was 1.4 (14%) for small to medium-sized shade structures. When the calculated PFs of 27 and 32 for the large shade structure are included (Figure 4: depicted by two unfilled circles) the MAE increases to 1.7 (16%) because the difference between PFs is greater for the large structure. This is likely to be due to the sky view for the large structure being comprised of the portion of the sky lower toward the horizon, where the diffuse UV may not be isotropic [64]. Consequently, the proposed method is suitable for small to medium-sized shade structures with a SVF of at least 8%.

As the PF of a structure is a function of SZA (affecting the shade pattern), the PFs were also evaluated at the centre of the small and medium structures on a cloud free day at approximately noon and also between approximately 10 am to noon. The PF at noon represent the maximum PF for each structure for that season. The PF for the small structure decreased from approximately 11 to 97 as SZA increased from 7^o (11.56 am in summer) to 47^o (Figure 5) with both the passage

of time and with the seasons. For the small and medium-sized structures, the calculated PF from mid-morning to noon demonstrates that the proposed method can be used at times other than noon, when the relative proportion of diffuse to direct UV is higher. Additionally, the PF for a given structure can be calculated in different seasons as the proportion of diffuse UV changes with the SZA.

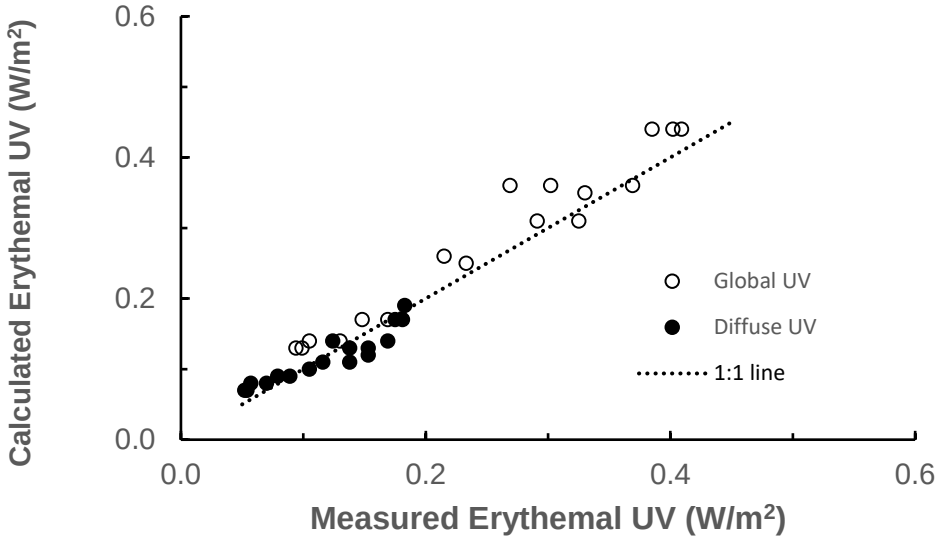

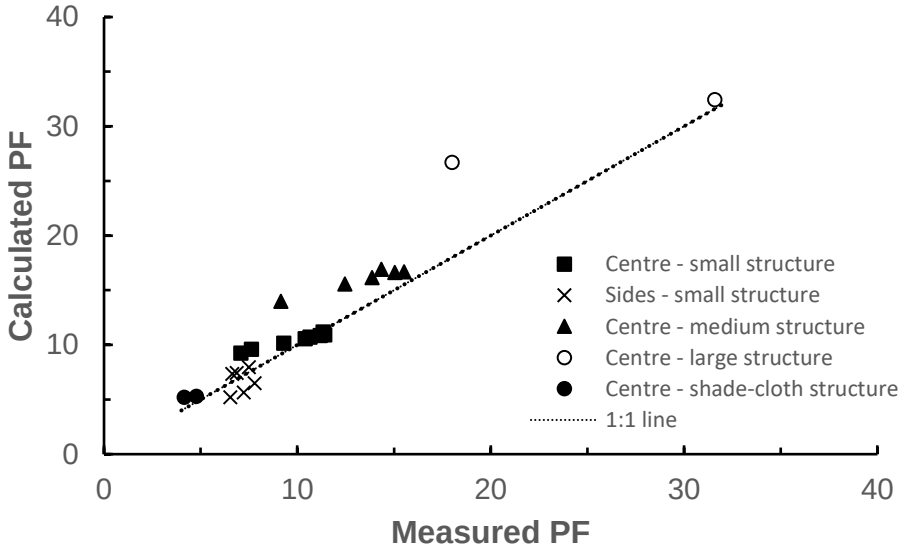

Figure 4 – Comparison of the calculated and measured global UV and diffuse erythemal UV irradiances (top graph) and comparison of the calculated Protection Factor (PF) versus measured PF (bottom graph), along with the 1:1 lines.

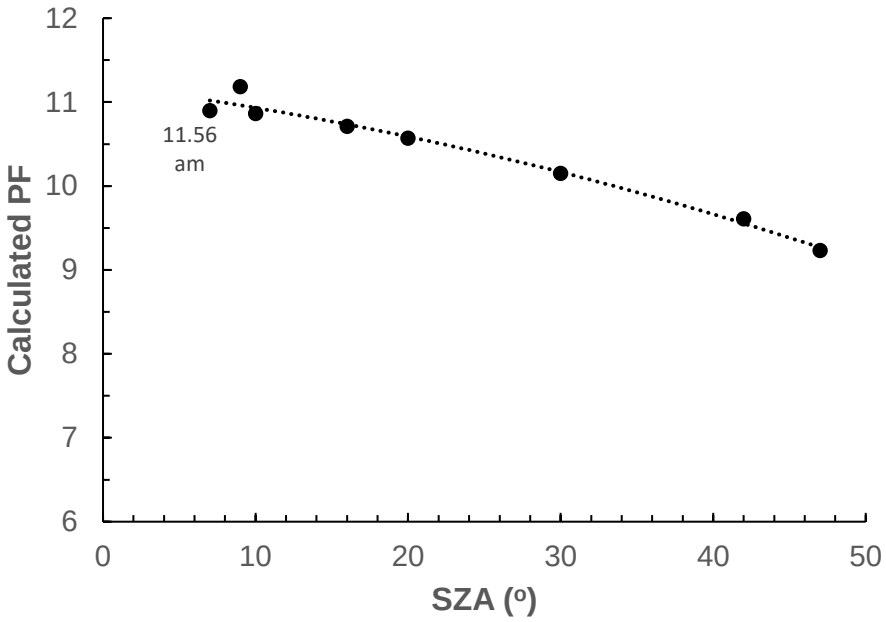

Figure 5 – The calculated PF at the centre of and 90 cm above the ground of the small structure at the different solar zenith angles (SZAs). The smallest SZA for this data is close to noon in summer and is shown as 11.56 am.

4. Conclusion

The proposed method has been tested in the field on four shade structures demonstrating its utility for calculating the PF of built small to medium-sized shade structures with a SVF greater than 0.08 (8%). The proposed method was developed for determining PF at 90 cm above ground-level in the centre of different shade structure designs with SVF ranging from 4.6% to 15.4%. Three of the structures had a thin metal roof and the fourth had shade-cloth. The SVF, albedo of the relevant surfaces, SZA (influences relative proportion of diffuse UV), measurement position beneath the

structure, and the UV-transmittance of the roof material (influenced by the age, stretch and weathering of the material) were taken into account. The proposed method was validated by comparing calculated and measured PFs across SZAs ranging from 7^{o} to 49^{o}. The MAE between calculated and measured PF for small and medium structures was 1.4 (14%), increasing to 1.7 (16%) if the large structure was included. Given the larger difference in calculated and measured PFs obtained for the large structure, the proposed method is only recommended for small to medium shade structures with a SVF of at least 8%.

Further research is required to confirm that the method works irrespective of time of year, time of day and the type of shade structure. Future testing of this method will determine its reliability under different albedos, SZA, temporal and seasonal conditions as well as for a broad range of shade structure sizes and designs with roofing materials exhibiting different UV-transmittance characteristics, both with and without side protection (positioned at different compass directions). Comparing PFs for different types of built structures will require measurement position beneath the structure, height above ground-level and SZA to be standardized.

The proposed method should inform the shade structure design process, resulting in newly constructed shade structures in public and community settings offering higher PFs than previous designs. It will enable the amount of UV protection provided by built shade structures in schools, early childhood settings and other public settings to be more readily determined by non-scientists with access to any smartphone device and some relatively inexpensive and widely-available tools. This research makes the determination of the PF of built shade simpler for both shade builders and the general public to carry out, when previous approaches were prohibitive because of the cost of

the UV meter required and the skills required to use one. Shade builders who use our easy to follow approach are likely to become better informed about the relative merits of various shade structure designs and the factors that influence their effectiveness, while government, sporting, school and community organisations who use our model will become more discerning and informed purchasers of built shade. . The proposed method could be used to provide an assurance of quality of shade that planned structures are expected to provide. Further automation of the method (e.g. developing a smartphone app) would make using the proposed method even easier and would likely facilitate its wide-spread adoption. Funders of shade could positively influence the shade industry in this direction by making it mandatory for shade builders quoting on shade provision to provide some assurance/guarantee of shade quality in terms of anticipated PF. If applicants seeking funding for additional shade were also expected to measure the PF of their existing shade structures using this method, it would also inform the distribution of limited shade funding to those who provide the highest PF. It is apparent from these applications alone that the proposed method has the potential to vastly improve communication about the quality of shade of planned structures and may form the basis of a quality assurance framework for the shade creation industry. Consequently, this research has the potential to influence the development of improved industry standards for shade creation.

Funding: This research did not receive any specific grant from funding agencies in the public, commercial, or not-for-profit sectors.

References

[1] World Health Organisation, 2017, Ultraviolet radiation and the INTERSUN programme, http://www.who.int/uv/sun_protection/en/ (accessed June 2017).

[2] Doran, C.M., Ling, R., Byrnes, J., Crane, M., Searles, A/. Perez, D. & Shakeshaft, A. 2015, "Estimating the economic costs of skin cancer in New South Wales, Australia," *BMC Public Health*, 15:952, doi.org/10.1186/s12889-015-2267-3

[3] Australian Institute of Health and Welfare, 2017. Summary pages for selected cancers 2017, http://www.aihw.gov.au/cancer/cancer-in-australia-2017/summary-pages-for-selected-cancers/#t17 (accessed August 2017).

[4] Fransen, M., Karahalios, A., Sharma, N., English, D.R., Giles, G.G. & Sinclair, R.D., 2012, "Nonmelanoma skin cancer in Australia," *Medical Journal Australia*, vol.197, pp.565–568.

[5] American Cancer Society, 2018, Cancer facts and figures 2018, https://www.cancer.org/research/cancer-facts-statistics/all-cancer-facts-figures/, (accessed June, 2018).

[6] Neidecker, M.V., Davis-Ajami, M.L., Balkrishnan, R. & Feldman, S.R. 2009, "Pharmacoeconomic considerations in treating actinic keratosis," *Pharmacoeconomics*, vol.27, pp.451–64.

[7] Whiteman, D. 2014, Inquiry into skin cancer in Australia, Submission to Parliamentary Inquiry, http://www.aph.gov.au/Parliamentary_Business/Committees/House/Health/Skin_Cancer/Submissions (accessed June 2017).

[8] SunSmart®, 2017, Skin cancer facts and stats, http://www.sunsmart.com.au/about/skin-cancer-facts-stats (accessed June 2017)

[9] SunSmart®, 2017, UV and sun protection, http://www.sunsmart.com.au/sun_protection (accessed June 2017).

[10] Parsons, P., Neale, R., Wolski, P. & Green, A. 1998, "The shady side of solar protection," *Medical Journal of Australia*, vol.168, pp.327-330.

[11] Gies, P., Makin, J., Dobbinson, S., Javorniczky, J., Henderson, S., Guilfoyle, R. & Lock, J. 2013, "Shade provision for toddlers at swimming pools in Melbourne," *Photochemistry and Photobiology*, vol.89, pp.968-973.

[12] Boyers, L.N., Karimkhani, C., Gamble, R. & Dellavalle, R.P. 2014, "Novel and promising sun safety interventions: UV photography and shade structures," *OA Dermatology*, Mar 09, vol.2(1), pp.1-6.

[13] Horner, M., Rhode-Barbarigos, L. & Adriaenssens, S, 2014, "Site-specific louvered shells for shading harmful ultraviolet radiation," *Building and Environment*, vol.78, pp.14-22.

[14] Diffey, B.L. 1980, "Ultraviolet radiation physics and the skin," *Physics in Medicine and Biology*, vol.25, pp.405-426.

[15] Turnbull, D. & Parisi, A.V. 2005, "Increasing the ultraviolet protection provided by shade structures," *J Photochem Photobiol B: Biol.* vol. 78, pp.62-67.

[16] Gong, F., Zeng, Z, Zhang, F., Li, X., Ng, E. & Norford, L.K. 2018, "Mapping sky, tree, and building view factors of street canyons in a high-density urban environment," *Building and Environment*, vol.134, pp.155-167.

[17] Middel, A., Lukasezyk, J., Maciejewski, R., Demuzere, M. & Roth, M. 2018, "Sky View Factor footprints for urban climate modelling," *Urban Climate*, vol.25, pp.120-134.

[18] Zeng, L., Lu, J., Li, W. & Li, Y. 2018, "A fast approach for large-scale Sky View Factor estimation using street view images," *Building and Environment*, vol.135, pp.74-84.

[19] Li, X., Ratti, C. & Seiferling, I. 2018, "Quantifying the shade provision of street trees in urban landscape: A case study in Boston, USA, using Google Street View," *Landscape and Urban Planning*, vol.169, pp.81-91.
[20] Australian Standard, AS 4174-2018, Knitted and woven shade fabrics, https://www-saiglobal-com.ezproxy.usq.edu.au/online/autologin.asp (accessed April 2018).
[21] SunSmart®, 2017, Shade audit, http://www.sunsmart.com.au/shade-audit/ (accessed May 2017).
[22] SunSafe Nova Scotia, 2006, Summer Sun Safety Program: How to Conduct a Shade Audit, http://www.cancercare.ns.ca/site-cc/media/cancercare/Shade_Audit_Guide.doc (accessed August 2017).
[23] Gage, R., O'Toole, C., Robinson, A., Reeder, A., Signal, L. & Mackay, C. 2018, "Wellington Playgrounds Uncovered: An Examination of Solar Ultraviolet Radiation and Shade Protection in New Zealand," *Photochemistry and Photobiology*, vol.94, pp.357-361.
[24] WebShade, nd, WebShade, Balmain, Australia, http://www.webshade.com.au/index.html (accessed May 2017).
[25] Moise, A.F. & Aynsley, R. 1999, "Ambient ultraviolet radiation levels in public shade settings," *International Journal of Biometeorology,* vol.43, pp.128-138.
[26] Downs, N, Parisi, A.V., Turner, J. & Turnbull, D. 2008, "Modelling ultraviolet exposures in a school environment," *Photochemical and Photobiological Sciences,* vol.7, pp.700-710.
[27] Moise, A.F., Buttner, P.G. & Harrison, S.L. 1999, "Sun exposure at school," *Photochemistry and Photobiology,* vol.70, pp.269-274.
[28] Turnbull, D.J. & Parisi, A.V. 2003, "Spectral UV in public shade settings," *Journal Photochemistry and Photobiology B: Biology*, vol.69, pp.13-19.
[29] Turnbull, D.J. & Parisi, A.V. 2004, "Annual variation of the angular distribution of the UV beneath public shade structures," *Journal Photochemistry and Photobiology B: Biology,* vol.76, pp.41-47.
[30] Gies. P. & Mackay, C. 2004, "Measurements of the solar UVR protection provided by shade structures in New Zealand primary schools," *Photochemistry and Photobiology*, vol.80, pp.334-339.
[31] Parisi, A.V., Eley, R., Downs, N. 2012, "Determination of the usage of shade structures via a dosimetry technique," *Photochemistry and Photobiology,* vol.88, pp.1012-1015.
[32] EPA (United States Environmental Protection Agency), 2017, Shade Planning for America's Schools, http://www.epa.gov/sunsafety/shade-planning-americas-schools (accessed June 2017).
[33] Cancer Council NSW, 2013, Guidelines to Shade, https://www.cancercouncil.com.au/wp-content/uploads/2011/04/Guidelines_to_shade_WEB2.pdf (accessed May 2017).
[34] SunSmart Victoria, 2015, Shade Guidelines, https://www.sunsmart.com.au/downloads/resources/brochures/shade-guidelines.pdf (accessed June 2017).
[35] Turner, D., Harrison, S.L., Buettner, P., Nowak, M. 2014, "Does being a "SunSmart School" influence hat-wearing compliance? An ecological study of hat-wearing rates at Australian primary schools in a region of high sun exposure," *Preventive Medicine*, vol.60, pp.107-114.
[36] Dobbinson, S.J., White, V., Wakefield, M.A., Jamsen, K.M., White, V., Livingston, P.M., English, D.R. & Simpson, J.A. 2009, "Adolescents' use of purpose built shade in secondary schools: Cluster randomised controlled trial," *British Medical Journal,* vol.338, pp.1-6.

[37] Hwang, R., Lin. T. & Matzarakis, A. 2011, "Seasonal effects of urban street shading on long-term outdoor thermal comfort," *Building and Environment*, vol.46, pp.863-870.
[38] Makaremi, N., Salleh, E., Jaafar, M. Z. & GhaffarianHoseini, A. 2012, "Thermal comfort conditions of shaded outdoor spaces in hot and humid climate of Malaysia," *Building and Environment*, vol.48, pp.7-14.
[39] Watanabe, S. & Ishii, J. 2016, "Effect of outdoor thermal environment on pedestrians' behavior selecting a shaded area in a humid subtropical region," *Building and Environment*, vol.95, pp.32-41.
[40] Cancer Council Qld, 2018, SunSmart shade initiative 2018, https://cancerqld.org.au/cancer-prevention/programs-resources/sunsmart-shade-initiative-2018/ (accessed June 2018).
[41] American Academy of Dermatology, 2018, Shade Structure Grant Program, http://www.aad.org/spot-skin-cancer/what-we-do/shade-structure-grant-program. (accessed June, 2018).
[42] Parisi, A.V. & Turnbull, D.J. 2014, "Shade provision for UV minimisation: a review," *Photochemistry and Photobiology*, vol.90, pp.479-490.
[43] Choice, 2014, Shady claims on shade sails, https://www.choice.com.au/outdoor/outdoor-entertaining/shade-cloths/articles/shade-cloth-investigation (accessed May 2017).
[44] Turnbull, D.J., Parisi, A.V. & Sabburg, J. 2003, "Scattered UV beneath public shade structures during winter," *Photochemistry and Photobiology*, vol.78, pp.180-183.
[45] Turnbull, D.J. & Parisi, A.V. 2006, "Effective shade structures," *Medical Journal of Australia*, vol.184, pp.13-15.
[46] Utrillas, M.P., Martinez-Lozano, J.A. & Nunez, M. 2010, "Ultraviolet radiation protection by a beach umbrella," *Photochemistry and Photobiology*, vol.86, pp.449-456.
[47] Grant, R.H. & Heisler, G.M. 2006, "Effect of cloud cover on UVB exposure under tree canopies: Will climate change affect UVB exposure," *Photochemistry and Photobiology*, vol.82, pp.487-494.
[48] Parisi, A.V., Willey, A., Kimlin, M.G. & Wong, J.C.F. 1999, "Penetration of solar erythemal UV radiation in the shade of two common Australian trees," *Health Physics*, vol.76(6), pp.682-686.
[49] Geoscience Australia, 2015, "Compute Sun and Moon Azimuth & Elevation," http://www.ga.gov.au/geodesy/astro/smpos.jsp (accessed August, 2017).
[50] Parisi, A.V., Downs, N., Igoe, D. & Turner, J. 2016, "Characterisation of cloud cover with a smartphone camera," *Instrumentation Science and Technology*, vol.44, pp.23-34, DOI:10.1080/10739149.2015.1055577.
[51] Microsoft, nd, Image Composite Editor, USA, https://www.microsoft.com/en-us/research/product/computational-photography-applications/image-composite-editor/ (accessed June 2017).
[52] Lindberg, F. & Holmer, B. 2010, Sky View Factor Calculator User Manual Version 1.1, University of Gothenburg, Sweden. http://www.gu.se/digitalAssets/1337/1337400_skyviewfactorcalculator-user-manual.pdf (accessed January 2017).
[53] MathWorks®, 2017, MATLAB Compiler, Massachusetts, USA. https://au.mathworks.com/products/compiler/mcr.html (accessed May 2017).
[54] Steyn, D.G. 1980, "The calculation of view factors from fisheye-lens photographs: Research Note," *Atmosphere-Ocean*, vol.18(3), pp.254-258, DOI: 10.1080/07055900.1980.9649091

[55] Johnson, G.T. & Watson, I.D. 1984, "The determination of view-factors in urban canyons," *Journal Climate and Applied Meteorology*, vol.23, pp.329-335.
[56] CIE (International Commission on Illumination) 1998, Erythema reference action spectrum and standard erythema dose, *CIE S007E-1998*, CIE Central Bureau, Vienna, Austria.
[57] Grant, R.H. 1997, "Biologically active radiation in the vicinity of a single tree," *Photochemistry and Photobiology*, vol.65, pp.974-982.
[58] Feister, U. & Grewe, R. 1995, "Spectral albedo measurements in the UV and visible region over different types of surfaces," *Photochemistry and Photobiology*, vol.62, no.4, pp.736-744.
[59] McKenzie, Kotkamp & Ireland 1996, "Upwelling UV spectral irradiances and surface albedo measurements at Lauder, New Zealand", *Geophysical Research Letters*, vol.23, pp.1761-1764.
[60] Diffey, B.L., Green, A.T., Loftus, M.J., Johnson, G.J. & Lee, P.S. 1995, "A portable instrument for measuring ground reflectance in the ultraviolet," *Photochemistry and Photobiology*, vol.61, no.1, pp.68-70.
[61] Turner, J. & Parisi, A.V. 2018, "Ultraviolet radiation albedo and reflectance in review: The influence to ultraviolet exposure in occupational settings," *International Journal of Environmental Research and Public Health*, vol.15, 1507, doi:10.3390/ijerph15071507
[62] Deo, R, D., Downs, N., Parisi, A,V., Adamwoski, J.F. & Quilty, J.M. 2017, "Very short-term reactive forecasting of the solar ultraviolet index using an extreme learning machine integrated with the solar zenith angle," *Environmental Research*, vol.155, pp.141-166.
[63] Mayer, B. & Kylling, A. 2005, "The libRadtran software package for radiative transfer calculations – description and examples of use," *Atmospheric Chemistry and Physics*, vol.5, pp.1855-1877.
[64] Grant, R.H., Heisler, G.M. & Gao, W. 1997, "Clear sky radiance distributions in ultraviolet wavelength bands," *Theoretical and Applied Climatology*, vol.56, pp.123-135.